Simulation of counterflow nonpremixed flame with electric fields

Jinwoo Son*, Jin Park, Min Suk Cha
King Abdullah University of Science and Technology (KAUST), Physical Science and Engineering Division (PSE), CCRC
Thuwal, Saudi Arabia

1 Introduction

The numerical studies of the electric fields on reacting flows have been studied over a couple of decades [1-4]. The electric field can generate the ionic wind due to space charges produced by chemi-ionization in a hydrocarbon flame. The advantages of applying electric fields are reducing soot [5, 6] and stabilizing flames [7, 8]. To simulate a flame under externally applied fields, we developed a multi-physics numerical code by adding Poisson's equation to solve electric field, transport modeling due to the ambipolar diffusion, and chemi-ionization chemistry on the conventional reacting flow solvers.

The novel points of this study were i) a chemical mechanism for the accurate perdition of CH and ii) the transport model of the electron. Ions and electrons are generated via a chemi-ionization reaction; CH radicals and O radicals produce the cation and electrons in the flame ($CH + O \rightleftharpoons CHO^+ + e^-$). Thus, predicting the accurate CH formation was essential to properly simulate the charged species in hydrocarbon flames. The diffusion coefficient and mobility of the electron were calculated by solving the Boltzmann equation based on mean cross-sections as a function of electron energy. To obtain the cross-sections, binary cross-sections colliding with the neutral species at a given reduced field (E/n) were necessary, which could be found in the LXCat [9].

Previous studies have employed the thermal equilibrium assumption for the electron transport model and used a simplified chemi-ionization reaction [1-3]. The electron temperature was assumed to be the same as the gas temperature in the thermal equilibrium. We plotted the binary cross-section of the electron in Fig. 1. The thermal equilibrium assumption was valid for a very narrow range of temperature only (0 – 0.3 eV). On the other hand, the electron temperature of the present study could be up to 2.3 eV when a high voltage (2.5 kV) was applied. Therefore, the thermal equilibrium assumption should lead to a significant underprediction of the cross-section, and finally, an over-prediction of the electron transport should be occurred. In addition, the simplified chemical kinetics, excluding CH formation, inaccurately predicted the production of the charged species (CHO^+ and electron) on a flame. Therefore, the numerical results showed not only inaccurate combustion characteristics but also a deviated electron flux.

In this regard, this study developed an improved numerical model by i) employing a nonequilibrium temperature of the electron, which was determined by the reduced electric field, ii) using a detailed

Correspondence to: jinwoo.son.1@kaust.edu.sa

kinetic mechanism to maintain the accurate level of CH radicals and, thus, CHO^+ formation. As a result, we obtained an improved prediction of the combustion characteristics (flame position and flow field) and the electric response (V−I trend and the electric field), compared to the previous studies.

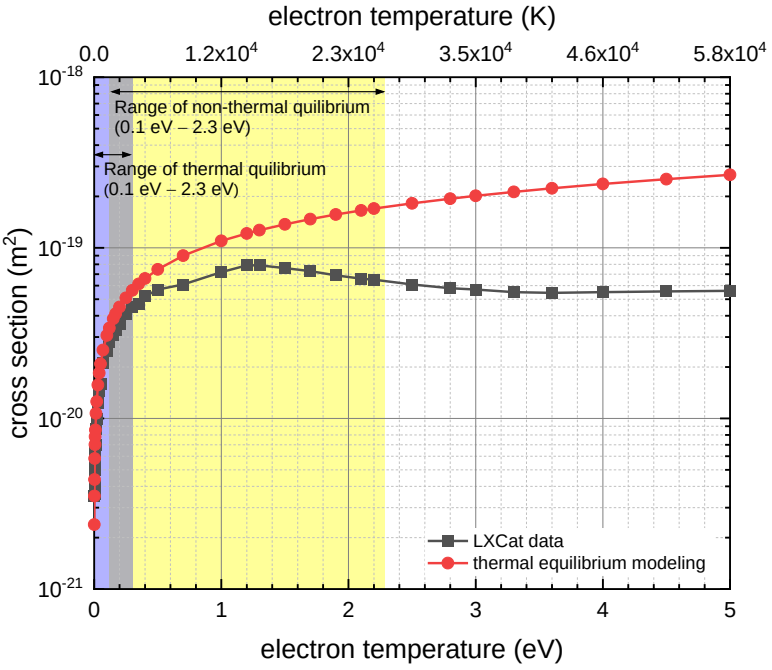

Figure 1: Binary cross-section (electron–N_2) of the electron with the thermal equilibrium assumption (from the previous study [1-3]) and the nonequilibrium approach (from the LXCat [9]).

2 Numerical methods

We developed a CFD method, based on OpenFOAM, to simulate a reacting flow under externally applied electric fields. We incorporated a Poisson equation solver for the electric field into the reactingFoam, a conventional solver for a combustion problem. A chemi-ionization mechanism was included in a combustion kinetic mechanism, because ions and electrons, generated in a flame, are the key messengers by transmitting the effect of the external electric field on them to an entire combustion field. The external electric field evacuates ions and electrons from a flame, resulting in distributed space charges along their passages. As a result of the local electric field and the space charges, the Lorentz force acting on the fluid can play a role in flow modification. Thus, the governing momentum equation must include the electric body force term. The governing equations consisted of the mass, the momentum, the species, and the energy as follows [1, 10, 11]:

$$\frac{\partial \rho}{\partial t} + \nabla \cdot (\rho \mathbf{U}) = 0, \tag{1}$$

$$\frac{\partial \rho \mathbf{U}}{\partial t} + \nabla \cdot (\rho \mathbf{U} \otimes \mathbf{U} + p\mathbf{I} - \boldsymbol{\tau}) = \rho \mathbf{g} + \mathbf{F}_e, \tag{2}$$

$$\frac{\partial \rho Y_k}{\partial t} + \nabla \cdot (\rho \mathbf{U} Y_k + \mathbf{J}_k) = \dot{\omega}_k, \tag{3}$$

$$\frac{\partial \rho E_t}{\partial t} + \nabla \cdot (\rho \mathbf{U} E) = \nabla \cdot [-\mathbf{q} + (\boldsymbol{\tau} - p\mathbf{I}) \cdot \mathbf{U}] \\ - \rho \sum_k^n h_k \dot{\omega}_k + \rho g \mathbf{U}, \quad (4)$$

where ρ, $\mathbf{U}$, p, and $\boldsymbol{\tau}$ are the density, the velocity vector, the pressure, and the stress tensor, respectively.

The electric body force term, $\mathbf{F}_e$ (a summation of the Lorentz force acting on a unit fluid volume for all charged species), was added into the momentum equation.

$$\mathbf{F}_e = \sum_i^N (q_i e) n_i \mathbf{E}, \quad (5)$$

where n_i and q_i are the number density and the charge number of the charged species i, respectively, and e is the elementary charge, e = 1.602×10^{-19} C. The electric field, $\mathbf{E}$, can be obtained by the Gauss law ($\nabla \cdot \mathbf{E} = -\nabla^2 \boldsymbol{V}$).

In the species equation, Y_k, $\mathbf{J}_k$, and $\dot{\omega}_k$ indicated the mass fraction, the diffusion flux, and the net production rate for species k. The diffusion flux of neutral species was calculated by Fick's law ($\mathbf{J}_k = -\rho D_k Y_k$). Meantime, the diffusion flux of charged species needed to include the ambipolar diffusion due to the electric field, as shown below:

$$\mathbf{J}_i = -\rho D_i Y_i + \frac{q_i}{|q_i|} \rho Y_i \mu_i \mathbf{E}, \quad (6)$$

where D_i and μ_i are the diffusion coefficient and the mobility of charged species k, respectively. In the energy equation, E, is the total energy, $\mathbf{q}$, is the heat flux, and h_k is the enthalpy of formation for species k.

The diffusivities and the mobilities of the electron and the ions are necessary to calculate the diffusion flux in the species equation (Eq. 6). We calculated those transport coefficients by solving the Boltzmann equation based on binary cross-section published in the LXCat library at a given reduced field (E/n).

As mentioned previously, ions and electrons are generated via a chemi-ionization reaction. Thus, we employed the reduced mechanism based on Aramco 2.0 for the neutral species, maintaining the CH formation, a laminar burning velocity, and a flame temperature. The reactions involving those charged species were taken from the previous study [11]. Therefore, the chemical mechanism of this study, including the chemi-ionization, consists of 41 neutral and 11 charged species (four positive ions, six negative ions, and the electron).

We configured a 2D axisymmetric computational domain based on a previous study [1, 12], such that the jet diameter, burner distance, and mixture composition were the same as in the previous study. The fuel and oxidizer were diluted with nitrogen, and the composition was characterized by a stoichiometric mixture fraction, Z_{st}. To set the Z_{st} = 0.5, the volumetric fractions of the fuel and oxidizer were 0.14 and 0.56, respectively. The grid size was maintained at 25 μm in the interest area and increased radially up to 100 μm; meantime, the vertical grid size was fixed at 25 μm due to the vertically thin distribution of CH. The applied voltage (V_a) was increased up to 2.5 kV in both polarities. The negative polarity drove the electric field toward the fuel, and the positive polarity pulled the electric field in the direction of the oxidizer, respectively.

3 Results and discussions

The calculated V-I trend of this study well predicts the experiment as shown in Fig. 2. Our numerical result showed (i) quantitatively matched current response in the sub-saturated regimes for all applied voltages, (ii) the higher saturated current in positive V_a than that in the negative ones and (iii) decreased

saturation current in negative V_a. Although the saturated currents in both polarities underestimated the experimental values, the overall trend significantly improved than that from the previous studies, which failed to capture the different saturation currents between the polarity of V_a, and the phenomenon that the current decreases at the saturation voltage could not be found. Although the previous study [3] used GRI mech., and ion-chemistry generating CHO^+ from CH and O radicals, the simulation falsely predicted the current response due to the electron transport model with the thermal equilibrium assumption.

Therefore, in addition to considering H_3O^+, the other positive ions, such as $C_2H_3O^+$ and CH_5O^+, are essential to predict the current response in case of negative V_a; meanwhile, the electron transport critically affected the different saturation currents between the polarity of V_a.

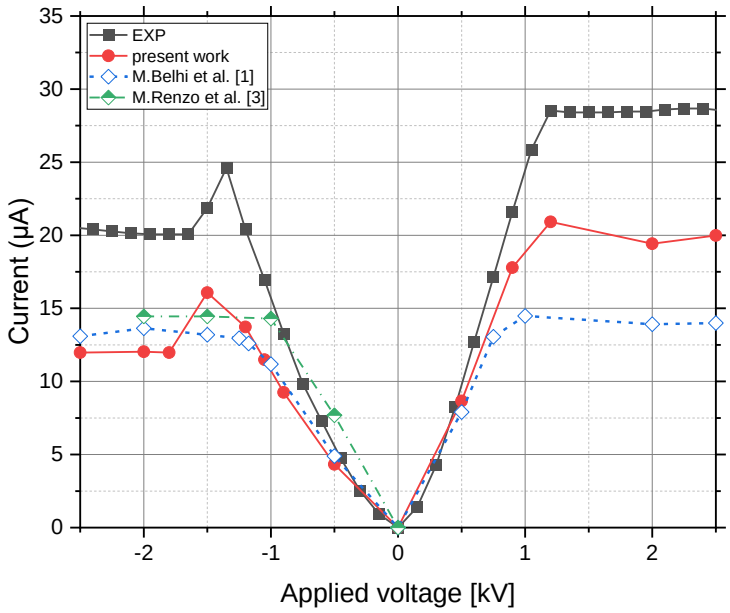

Figure 2 V-I trend for various modelings and experiment (solid line: measured and simulated current from the present work, dashed/dotted line: numerical results from the previous studies [1, 3]).

Based on the aforementioned findings, we suggested that the electric field comparison between the simulation and the experiment should be essential, since the local electric field determines electron transport and chemistry. We plotted the electric field at the sub-saturation/saturation voltage from the simulation and the experiments in Fig. 3. The calculated electric field at $V_a = -0.5$ kV showed quantitative/qualitative agreement with the experimental result. Despite the under-estimated electric field in the unburned region up to 22.8 % at y = 0.06 cm, we successfully showed a reasonable trend of the electric field as a result of our improved numerical modeling.

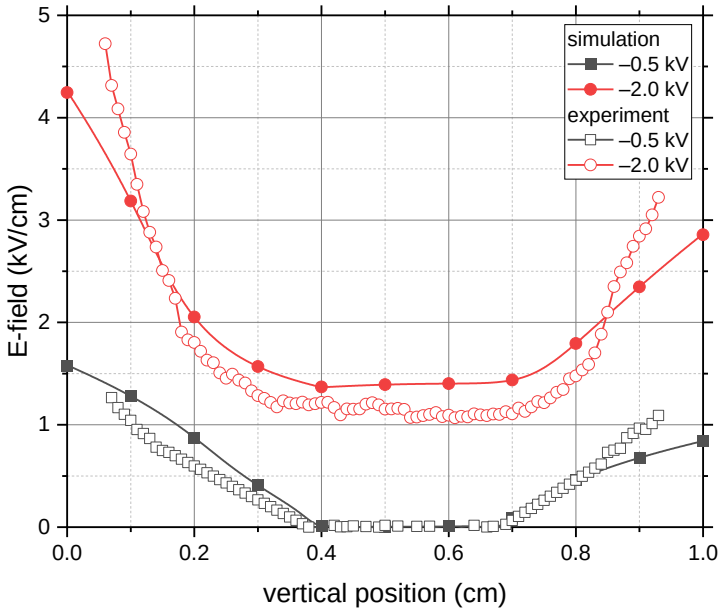

Figure 3 Electric field along the burner axis for the simulation and the experiment (sub-saturated regime at V_a = –0.5 kV, and saturated regime at V_a = –2 kV, respectively).

4 Conclusion

We performed the numerical study to investigate the effect of the electric field on 1D nonpremixed flame. The present study implemented the thermally nonequilibrium transport coefficients and a comprehensive ion-chemistry. We compared the simulated V-I characteristics with the previous studies and the experimental result. The electric field was also compared to the present numerical result. This study showed that; i) the newly applied transport model positively affected the saturation current for the respective polarity, and ii) the used nascent positive ion influenced the peak current behavior at the negative applied voltages. Therefore, we confirmed that the physically reasonable electron transport model was based on the nonequilibrium assumption. In addition, the simplified ion chemistry causes a significant uncertainty even in V-I analysis.

5 Acknowledgment

This study was supported by King Abdullah University of Science and Technology (KAUST), under award number BAS/1/1384-01-01. For computer time, this research used the resources of the Supercomputing Laboratory at KAUST.

References

[1] Belhi M, Lee BJ, Bisetti F, Im HG. (2017). A computational study of the effects of DC electric fields on non-premixed counterflow methane-air flames, J. Phys. D: Appl. Phys. 50.
[2] Belhi M, Lee BJ, Cha MS, Im HG. (2019). Three-dimensional simulation of ionic wind in a laminar premixed Bunsen flame subjected to a transverse DC electric field. Combust. Flame. 202: 90.
[3] Renzo MD, Urzay J, Palma PD, Tullio MD, Pascazio G. (2019). The effects of incident electric fields on counterflow diffusion flames. Combust. Flame. 193: 177.
[4] Xiong Y, Park DG, Lee BJ, Chung SH, Cha MS. (2016). DC field response of one-dimensional flames using an ionized layer model. Combust. Flame. 163: 317.

[5] Saito M, Arai T, Arai M. (1999). Control of soot emitted from acetylene diffusion flames by applying an electric field. Combust. Flame. 119: 356.
[6] Kono M, Carleton FB, Jones AR, Weinberg FJ. (1989). The effect of nonsteady electric fields on sooting flames. Combust. Flame. 78: 357.
[7] Kim MK, Ryu SK, Won SH, Chung SH. (2010). Electric fields effect on liftoff and blowoff of nonpremixed laminar jet flames in a coflow. Combust. Flame. 157: 17.
[8] Criner K, Cessou A, Louiche J, Vervisch P. (2006). Stabilization of turbulent lifted jet flames assisted by pulsed high voltage discharge. Combust. Flame. 144: 422.
[9] Pitchford LC, Alves LL, Bartschat K, Biagi SF, Bordage MC, Bray I, Brion CE, Brunger MJ, Campbell L, Chachereau A, Chaudhury B, Christophorou LG, Carbone E, Dyatko NA, Franck CM, Fursa DV, Gangwar RK, Guerra V, Haefliger P, Hagelaar GJM, Hoesl A, Itikawa Y, Kochetov IV, McEachran RP, Morgan WL, Napartovich AP, Puech V, Rabie M, Sharma L, Srivastava R, Stauffer AD, Tennyson J, Urquijo J, van Dijk J, Viehland LA, Zammit MC, Zatsarinny O, Pancheshnyi S. (2017). LXCat: an Open-Access, Web-Based Platform for Data Needed for Modeling Low Temperature Plasmas. Plasma Process Polym. 14.
[10] Poinsot T, Veynante D. (2005). Theoretical and numerical combustion. RT Edwards (ISBN . 1-930-21710-2)
[11] Prager J, Riedel U, Warnatz J. (2007). Modeling ion chemistry and charged species diffusion in lean methane–oxygen flames. Proc. Combust. Inst. 31: 1129.
[12] Park DG, Chung SH, Cha MS. (2016). Bidirectional ionic wind in nonpremixed counterflow flames with DC electric fields. Combust. Flame. 168: 138.